Modelling and control of hybrid UPS system with backup PEM fuel cell/battery

Yuedong Zhan [a,*], Hua Wang [a], Jianguo Zhu [b]

[a] Department of Automation, Kunming University of Science and Technology, Kunming 650093, China
[b] Faculty of Engineering, University of Technology, Sydney, NSW 2007, Australia

ARTICLE INFO

ABSTRACT

This paper describes the dynamics modelling of a practical and cost-effective DC/DC converter, DC/AC inverter and AC/DC rectifier for an uninterruptible power supply (UPS) system with backup proton exchange membrane fuel cell (PEMFC) and battery. Furthermore, a dynamics modelling and intelligent comprehensive controller for the PEMFC is designed according to the change of the load, while the energy storage elements, such as battery and supercapacitor, are chosen to compensate the slow dynamic response of PEMFC and to meet the sudden peak load energy demand. The power converters based on dynamic modelling and controllers designed by feedback control theory can supply high quality power with flexible conversion functions, leading to the establishment of reliable power management for UPS applications. Finally, a suitable control strategy and technique, capable of coping with the change of the load for PEMFC and realising the energy management strategy of hybrid UPS system, is implemented. The performances of the proposed power converters and PEMFC generating system are evaluated by experimental results, showing that the developed hybrid UPS system with backup PEMFC and battery power sources is suitable for industry applications.

1. Introduction

Uninterruptible power supply (UPS) technologies can provide energy solutions to some customers such as computers and communication equipments that are more cost effective, more environmentally friendly, or provide a clean output voltage with low total harmonic distortion (THD) for both linear and nonlinear loads, high efficiency, great reliability and fast transient response for sudden power grid failure and load changes, and avoiding financial loss and data loss than conventional solutions. Thanks to high electrical efficiency, flexibility with respect to power and capacity, long lifetime and no pollutions, the fuel cells, including the proton exchange membrane fuel cell (PEMFC), are rapidly becoming a significant power source in the design and development of UPS [1,2].

The integration of fuel cells with UPS would become a potential market application for extended run-time UPS. To a long-term demand and more power capacities of UPS, fuel cells systems appear as strong contenders to replace batteries, especially in grid-connected applications where good quality reliable power supply is required, or interruptions could last long time, e.g. over 8 h [3,4]. However, limited by their inherent characteristics, the fuel cells have a long start-up time (usually several seconds to minutes) and poor response to instantaneous power demands.

Compared with fuel cells, lithium rechargeable batteries have a rapid transient response without any warm up or start-up time, and their specific power capability is also much higher than that of fuel cells. Combination of fuel cells with small capacity of batteries or supercapacitors yields hybrid power sources that make the best use of the advantages of each individual device and may meet the requirements for the above mentioned applications regarding both high power and high energy densities [5,6]. On the other hand, the UPS system employing a PEMFC as the main power source keeps adopting the battery or supercapacitor for protecting the PEMFC, in order to keep the water content balance, avoid excessive use and the reactants starvation of the PEMFC and feed power smoothly to the external load.

As the applications of backup power source for UPS, a dynamic model and efficient control of PEMFC are necessary during the normal operation of PEMFC system, when the operating condition varies or an operation with alternating loads. The power response of the PEMFC generating system depends mainly on the interaction of the PEMFC stack and the peripheral components like hydrogen and air supply, mass flow, temperature and pressure control, heat and water management. Hence, the control objectives for a hybrid UPS system are to maintain efficiency and to avoid degradation by guaranteeing appropriate temperature, mass flows and partial pressures of the reactants across the electrodes [7,8].

Recently, some of researches have concentrated on modelling and control of hybrid UPS systems. In [2,9,10] the development

* Corresponding author. Tel.: +86 871 6733875; fax: +86 871 3304192.
E-mail addresses: ydzhan@163.com (Y. Zhan), wanghua65@163.com (H. Wang), joe@eng.uts.edu.au (J. Zhu).
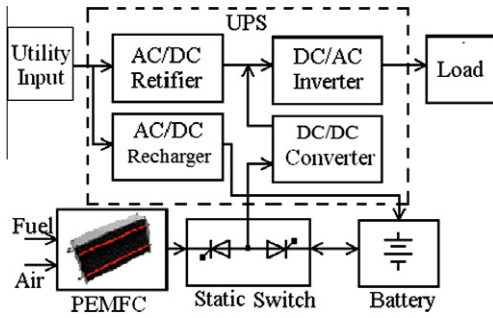
Fig. 1. Hybrid UPS system with backup PEMFC and battery.

and control strategies for hybrid UPS system has been presented. In [11] a 1 kVA fuel cell powered, line-interactive UPS system that employed modular (fuel cell and power converter) blocks has been developed using two commercially available PEMFC (25–39 V, 500 W) modules together with suitable DC/DC and DC/AC power electronic converter modules and a supercapacitor module that was also used to compensate for the instantaneous power fluctuations and to overcome the slow dynamics of the fuel processor (reformers). In [12] an UPS system based on hydrogen technologies has been designed, manufactured and tested, which consists of a PEMFC running on hydrogen and oxygen, a gas storage section and a water electrolysis for hydrogen and oxygen production. In [13] a technological solution for the association in parallel of two (or more) PEMFC stacks has been proposed. Different types of architectures for multi-stack fuel cells were introduced, and a suitable power converter interface has been designed.

In this paper, based on the concepts adopting matured technology for the components of the hybrid UPS system, the double charging of the battery through the AC/DC charger or the PEMFC, and being easy to develop serial products, an industrial hybrid UPS system with backup PEMFC and battery power sources is developed in order to supply long-time load with a typical power (300 W, 220 VAC, 50 Hz). The proposed power converters, such as AC/DC rectifier, DC/DC converter, and DC/AC inverter, are designed, modelled, controlled and evaluated through the experimental tests on a laboratory prototype. In order to improve the performance of the PEMFC, an intelligent comprehensive controller is also proposed. Fig. 1 illustrates schematically the structure of a single-phase high-frequency cost-effective hybrid UPS system with a backup PEMFC and battery power sources.

2. Dynamic modelling of hybrid UPS system

The dynamic modelling of a hybrid UPS system is an important issue that needs to be carefully addressed. Because a PEMFC model allows a better comprehension of the parameters affecting the performance of single fuel cells and fuel cell systems [14]. Generally, a power electric component consists of the power converter, PWM modulator, gate driver and feedback controller. According to the knowledge of control theories, the static and dynamic performances of power converters are intensely related to the design of feedback controller. Before designing a controller, therefore, the dynamic models of the power converter and PWM modulator must be gained. However, a good model should consider both accuracy and operating frequency of control chips. In this paper, the power electric components of the hybrid UPS system comprise AC/DC rectifier, DC/DC converter, and DC/AC inverter, while the electrochemical component is PEMFC and the energy storage component is battery. The mathematical models describing the dynamic behaviour of each of these components will be given below.

2.1. PEMFC modelling

2.1.1. Polarisation curve model

The model of PEMFC used in this paper is based on the dynamic PEMFC stack model developed and validated in [15]. Because of the activation loss voltage $V_{actLOSS}$, Ohmic loss voltage $V_{OhmicLOSS}$, concentration loss voltage $V_{concLOSS}$ and leakage loss voltage (internal current) $V_{leakLOSS}$, the mathematical polarisation curve model of the PEMFC stack will be

$$V_{stack} = V_{reversible} - V_{actLOSS} - V_{OhmicLOSS} - V_{contLOSS} - V_{leakLOSS}$$
$$= V_{reversible} - N_{CELL}\left\{\frac{RT}{\alpha F}\ln\left(\frac{i+i_n}{i_0}\right) + R_{Ohmic}(i+i_n) + \frac{RT}{nF}\ln\left[\frac{i_L}{i_L-(i+i_n)}\right]\right\} \quad (1)$$

where $V_{reversible}$ is the reversible voltage (V); N_{cell} the number of cells in a PEMFC stack; α is the transfer coefficient; n the number of electrons per molecule of H_2 = 2 electron per molecule; R the universal gas constant (J/mol K); T the stack temperature (K); F the Faraday's constant (C/mol); R_{Ohmic} the area-normalised resistance, also known as area specific resistance (ARS) of the PEMFC measured (Ω cm^2); i_0 the exchange current density (A/cm^2); i_L the limiting current density at which the cell voltage will fall rapidly (A/cm^2); i_n the internal current or parasitic current that is wasted (A/cm^2); and i is the PEMFC stack current density (A/cm^2).

The reversible voltage at varying temperature and pressure can be expressed as

$$V_{reversible} = N_{cell} \times 1.23 + (4.308 \times 10^{-5})T \times \ln\left[\frac{P_{H_2}(P_{O_2})^{\frac{1}{2}}}{P_{H_2O}}\right]$$
$$- N_{cell} \times (8.453 \times 10^{-4})(T - 298.15) \quad (2)$$

where P_i is the partial pressure of species i (H_2, O_2/air, and liquid water) (kPa), respectively.

According to the conservation of energy, the ideal gas law, the proportional relationship between the gas outlet flow through a valve and the partial pressure, and Faraday's law, P_{H_2}, P_{O_2} and P_{H_2O} can be reconstructed in the s domain as

$$P_{H_2} = \frac{1/k_{H_2}}{1 + \tau_{H_2}s}(Q_{H_2}^{in} - 2k_rI) \quad (3)$$

$$P_{O_2} = \frac{1/k_{O_2}}{1 + \tau_{O_2}s}(Q_{O_2}^{in} - k_rI) \quad (4)$$

$$P_{H_2O} = \frac{1/k_{H_2O}}{1 + \tau_{H_2O}s}(Q_{H_2O}^{in} + 2k_rI) = \frac{1/k_{H_2O}}{1 + \tau_{H_2O}}(2k_rI) \quad (5)$$

where

$$\tau_{H_2} = \frac{V_{an}}{k_{H_2}RT} \quad (6)$$

$$\tau_{O_2} = \frac{V_{cn}}{k_{O_2}RT} \quad (7)$$

$$\tau_{H_2O} = \frac{V_{cn}}{k_{H_2O}RT} \quad (8)$$

where τ_{H_2} and τ_{O_2} are the time constant of each gas (s); $Q_{H_2}^{in}, Q_{O_2}^{in}$ and $Q_{H_2O}^{in}$ the inlet flow rates of hydrogen, oxygen, and the water of the cathode (mol/s); k_{H_2}, k_{O_2} and k_{H_2O} each gas valve molar constant (kPa mol/s); k_r the modelling constant (mol/s A); V_{an} anode volume (m^3); V_{cn} cathode volume (m^3).

The inlet pressure of each gas can be calculated as

$$P_{H_2}^{in} = \frac{1}{1 + \tau_{H_2pneu}}(R_{H_2pneu}Q_{H_2}^{in} + P_{H_2}) \quad (9)$$

$$P_{O_2}^{in} = \frac{1}{1 + \tau_{O_2 pneu}}(R_{O_2 pneu} Q_{O_2}^{in} + P_{O_2}) \qquad (10)$$

where $P_{H_2}^{in}$ and $P_{O_2}^{in}$ are the inlet manifold or a pipe pressure of hydrogen and oxygen (kPa); $R_{H_2 pneu}$ and $R_{O_2 pneu}$ the pneumatic resistance of the hydrogen and oxygen manifold (Ω); $C_{H_2 pneu}$ and $C_{O_2 pneu}$ the pneumatic capacitance of the hydrogen and oxygen manifold (F); $\tau_{H_2 pneu}$ and $\tau_{O_2 pneu}$ the pneumatic time constant the hydrogen and oxygen manifold (s).

2.1.2. Thermal model

According to the Fourier's law of conduction, when involving internal heat generation due to electrical resistance, the rate of heat transferred by conduction in one-dimension through A is expressed by [16]

$$\frac{d^2 T}{dx^2} + \frac{q_{int}}{kA} = 0 \qquad (11)$$

where k is the thermal conductivity (W/m K), A the finite cross-sectional area (m^2), and q_{int} the rate of heat generation per unit volume (W).

In the PEMFC, the internal heat generation results from the electrical and ionic resistance as

$$q_{int} = i^2 R_{Ohmic} \qquad (12)$$

To three-dimensional steady state heat conduction, there is a non-linear equation:

$$\nabla(\nabla T) = 0 \qquad (13)$$

where ∇ is the differential operator, which is $\nabla = \frac{\partial}{\partial x} + \frac{\partial}{\partial y} + \frac{\partial}{\partial z}$.

To solve this equation, two boundary conditions (for each direction) must be given that describe the behaviour of the temperature at the system boundaries (constant temperature or prescribed flux).

In practice, if the entrance pressures of the hydrogen and air are constant, that is, if their flow rates are constant, which can be controlled, the nonlinear equation of the thermal model for the stack under the operating temperature can be expressed by

$$T(t) = g(U_{Fan}(t), T_{Air}(t)) = g(\bullet) \qquad (14)$$

where $U_{Fan}(t)$ is the blower velocity (rpm = revolutions per minutes) and $T_{Air}(t)$ is the air entrance temperature (K).
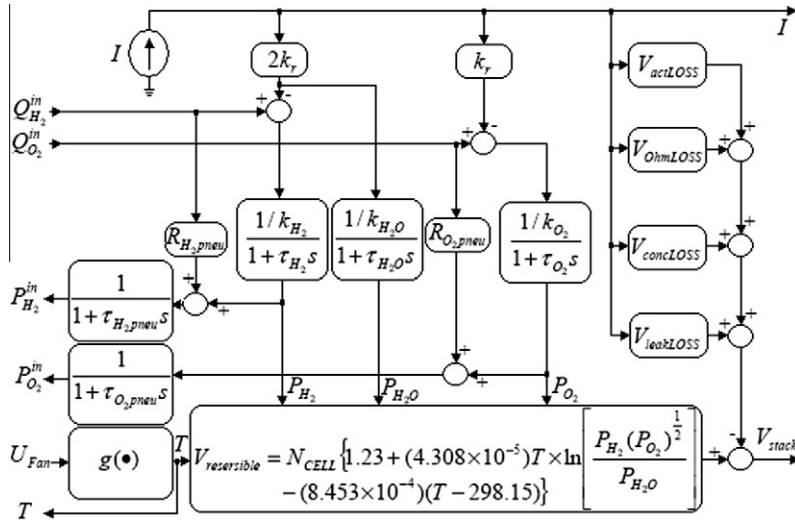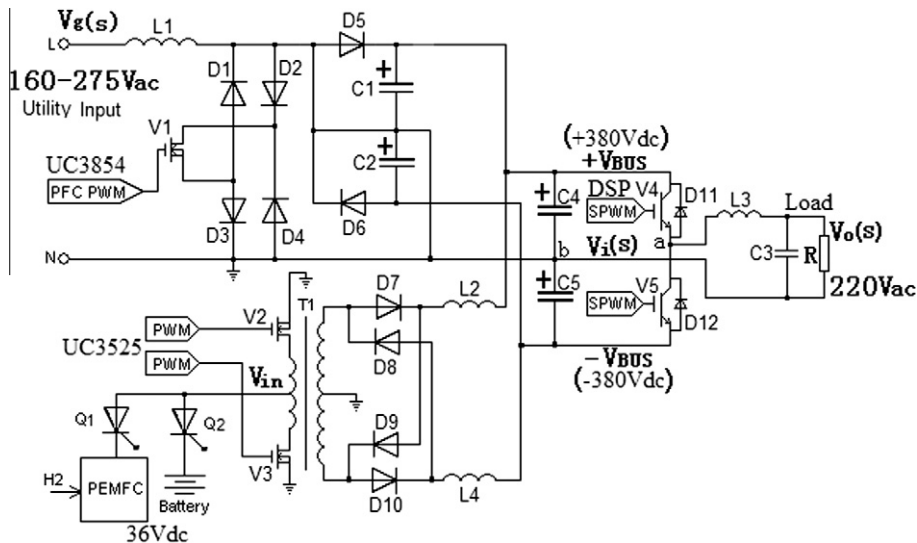

Fig. 2. PEMFC dynamic model.

Fig. 3. Power converters scheme for a hybrid UPS system.

2.1.3. Dynamic model of PEMFC

As mentioned above, a detailed dynamic model of the PEMFC is shown in Fig. 2. This model is based on the relationship between output voltage and the partial pressures of hydrogen, oxygen/air, water, and temperature and output current of the stack.

2.2. Modelling of power converters

According to the design concepts as mentioned above, the proposed topology of the power converters, or the power conditioners for the hybrid UPS system, is shown in Fig. 3. According to its functionality, the system can mainly be considered as composed by three main sections. The first one consists of a DC/DC converter whose principal task is to boost the rated output voltage 36 VDC of PEMFC and battery to a regulated voltages ±380 VDC. The second one is an AC/DC rectifier which rectifies the utility input voltage into ±380 VDC. The three sections is a DC/AC converter which generates a 50 Hz, 220 VAC output voltage.

A boost active power factor corrector (PFC) with 160–275 VAC input voltage and fixed output voltage (±BUS = ±380 VDC) is designed based on a high power factor pre-regular UC3854, which can make the input power factor (PF) of the AC/DC boost PWM rectifier be close to 1, restrict the input current's THD less than 5%, adopt the average current control and constant frequency control, and allow the frequency band of its current amplifier to be wide.

A general and practical DC/DC push–pull converter for the UPS hybrid system is designed based on a regulating pulse width modulator UC3525. The PEMFC and battery are two kinds of low-voltage and high-current power source, so their output voltage (36 VDC) should be boosted up to about ±380 VDC before the UPS DC/AC inverter converts them into a 220 V, 50 Hz AC source.

In the developed hybrid UPS system, by applying a TMS320F240 DSP, a DC/AC half-bridge inverter has been designed to supply the load with a pure sine wave, where the half-bridge inverter, LC filter and load are considered as the plant to be controlled. Through the sine pulse width model (SPWM) control principle, the DC/AC inverter can convert the ±380 VDC into a 220 VAC pure sine wave.

2.2.1. Modelling of AC/DC rectifier

The modelling approaches of the Boost AC/DC rectifier have the average switch network method, state space average method, and unifying circuit model method [17]. Although the AC/DC rectifier is a nonlinear, using the method of disturbance and linearisation, the small signal ac equations can be obtained. The state space average method is usually employed in power converters. However, the average switch network method is more convenient than the state space average method. The substance of the average switch network method is that the equivalent controlled source is firstly used to replace switch network; then, the disturbance and linearisation process is utilised; finally, the small signal ac model circuits can be obtained. The unifying circuit model method is perfect for basic DC/DC converter. Through the lookup table, when the parameters of AC/DC rectifier put into the unifying circuit model, the small signal ac model circuits can be gained. Fig. 4 shows the unifying circuit model of AC/DC rectifier.

According to the model, it is easy to deduce the transfer function from input voltage $V_g(s)$ to output voltage $v_{BUS}(s)$ and the transfer function from duty cycle signal $d(s)$ to output voltage $v_{BUS}(s)$.

$$\frac{v_{BUS}(s)}{V_g(s)} = \frac{D_1'}{L_1C_1s^2 + \frac{L_1}{R}s + D_1'^2} \tag{15}$$

$$\frac{v_{BUS}(s)}{d(s)} = \frac{D_1'V_{BUS}\left(1 - \frac{sL_1}{D_1'^2R}\right)}{L_1C_1s^2 + \frac{L_1}{R}s + D_1'^2} \tag{16}$$
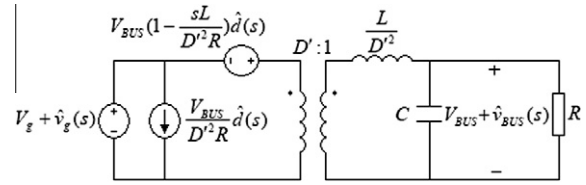

Fig. 4. Unifying circuit model of AC/DC rectifier.

where $D_1' = 1 - D_1$, D_1 is the duty cycle in a stable working point for AC/DC rectifier; L_1 the inductance (H); C_1 the capacitor (F); V_{BUS} is output BUS voltage (V); R the equivalent resistance of load (Ω).

On the other hand, the PWM modulator is to convert the control voltage $v_c(t)$ into the pulse sequence of duty cycle $d(t)$, and the modulator model can be determined by

$$\frac{d(s)}{v_c(s)} = \frac{1}{V_M} \tag{17}$$

where V_M is the peak value of sawtooth wave (V).

2.2.2. Modelling of DC/DC converter

The proposal DC/DC converter is a push–pull converter and works in the double state of polarity. Because the similar modelling method like AC/DC Boost rectifier, as mentioned above, can be used, this paper will ignore it.

When designed, it is important to effectively avoid the iron core saturation. Its circuit diagram is shown in Fig. 3. Since there are two switches V_2 and V_3, which work alternately, the output voltage V_{BUS} is doubled. Under the condition of the continuous current, the output voltage is calculated by the formula:

$$V_{BUS} = D_2NV_{in} \tag{18}$$

where N is the transformer turn ratio, D_2 the conduction duty cycle for DC/DC converter, $D_2 = 2Ton/T_S$, T_S the working cycle (s); V_{in} the input voltage (V), that is the voltages of the PEMFC stack and battery.

When the load current I_0 is not continuous, the output voltage is as follows:

$$V_{BUS} = \frac{V_{in}^2D_2^2N^2T_s}{4L_2I_0 + V_{in}D_2NT_S} \tag{19}$$

2.2.3. Modelling of DC/AC inverter

In the control model of inverter circuits, the pulses obtained by comparing reference sine wave $V_{in}\sin(\omega t)$ with triangular wave, which peak value is V_M', are used to control the power switch components. Simply, according to Fig. 3, as the equivalent series resistance r of the filter inductance is ignored, the transfers function between output voltage $V_o(s)$ and the voltage $V_i(s)$ of point a, and b is determined by

$$\frac{V_o(s)}{V_i(s)} = \frac{\frac{1}{\frac{1}{R}+C_3s}}{\frac{1}{\frac{1}{R}+C_3s} + L_3s} = \frac{1}{L_3C_3s^2 + \frac{L_3}{R}s + 1} \tag{20}$$

where L_3 and C_3 are the filter inductance (H) and capacitor (F) for AC/AC inverter, respectively.

Meanwhile, the transfers function from the modulator input to the inverter bridge output is

$$\frac{V_i(s)}{V_{in}(s)} = \frac{V_{BUS}}{V_M'} \tag{21}$$

By combining Eq. (20) and Eq. (21), the transfers function $\frac{V_o(s)}{V_{in}(s)}$ from the modulator input to the inverter output can be obtained as follows:

$$\frac{V_o(s)}{V_{in}(s)} = \frac{1}{L_3C_3s^2 + \frac{L_3}{R}s + 1} \frac{V_{BUS}}{V'_M} \tag{22}$$

2.3. Battery model

The battery stores energy in the electrochemical form, and is the most widely used device for energy storage in the variety of applications such as electric and hybrid electric vehicles and hybrid power systems. Because the dynamic modelling of a battery is extremely difficult and understanding what is going on in batteries requires several years of thorough research effort, in this paper, a simple battery model is introduced. The battery current I_{bat} as function of the required battery power P_{bat}, the internal resistance R_i and the open-loop voltage U_o is [18]:

$$U_{bat} = U_o - R_iI_{bat} \tag{23}$$

$$P_{bat} = U_{bat}I_{bat} \tag{24}$$

$$I_{bat} = \frac{U_o - \sqrt{U_o^2 - 4P_{bat}R_i}}{2R_i} \tag{25}$$

3. Controller design of hybrid UPS system

3.1. Intelligent comprehensive controller design of PEMFC

Aiming to conveniently collect the data, setup parameters for PEMFC, and properly choose the power, voltage and size of the PEMFC stack according to its cost, an intelligent comprehensive controller of the PEMFC generating system is designed as shown in Fig. 5. The data acquisition and control software have been developed and can be used to control the whole process of the PEMFC generating system and to measure and monitor the operational parameters, such as the work temperature, voltage and current, pressure, input and output mass flows, humidity of the hydrogen and air/oxygen, the voltage and current of the battery, water balance, and so on. The proposal intelligent comprehensive controller contains a 300 W, 63-cell, self-humidified, air-cooling and air breathing stack [19], a monitoring system and five control subsystems: power tracking controller, hydrogen pressure controller, hydrogen mass flow control (HMFC), air supply and thermal controller, and power switching controller. In Fig. 5, M is a multiplier, which is applied to calculate the output power of the PEMFC, and SCR$_1$ and SCR$_2$ are the silicon-controlled rectifiers (SCRs), which are used to switch the power sources between the PEMFC

and battery when the UPS starts up, the load increases sharply, the current is interrupted, or the utility grid power fails.

3.1.1. Power tracking controller

According to the real-time current and voltage measurements of PEMFC stack, the power (ranging from 12 to 330 W) can be firstly calculated. The output power of the fuel cell stack can be calculated by

$$P_{stack} = V_{stack}I \tag{26}$$

where P_{stack} is the output power (W), V_{stack} the output voltage (V), and I the output current of the stack (A).

Based on the load at that time, a power tracking controller is designed to continuously distribute the current or real-time power by using the setup value of the reference mass flow $Q_{H_2}^{ref}$ and $Q_{O_2}^{ref}$ of hydrogen and air and according to the stoichiometry radios of PEMFC. The mass flow rates of hydrogen and air for the stack can be calculated as follows.

3.1.1.1. Hydrogen mass flow rate.
At the standard conditions of the atmospheric pressure and 0 °C, the molar volume is [20]

$$V_m = \frac{RT}{P} = \frac{8.314 \times 278.15}{101,300} = 0.0224 \text{ m}^3/\text{mol} = 22.4 \text{ L/mol} \tag{27}$$

Therefore the reference volumetric flow rate of pure hydrogen consumption in standard litres per minute or SL/min is

$$Q_{H_2}^{ref} = 22.4 \times 60 \times \frac{IN_{cell}}{2F} \times S_{H_2} \tag{28}$$

where S_{H_2} is the stoichiometry radio of hydrogen, which is selected within 1.2–1.5.

3.1.1.2. Air mass flow rate.
Because the PEMFC stack selected is an air-breathing and air-cooling fuel cell, that is, air is passing through the cathode compartment in excess of oxygen exact stoichiometry, and the same air is used as a coolant. In the PEMFC generating system, air is supplied by three blowers that are used to cool the stack. The air volumetric mass flow rate in SL/min is [20]

$$Q_{O_2}^{ref} = 22.4 \times 60 \times \frac{M_{Air}IN_{cell}}{4F} \times S_{O_2} \tag{29}$$

where M_{Air} is the air mass (kg) and S_{O_2} is the required stoichometric radio, which is selected within 20–30.

According to the dynamic analysis of the PEMFC, if the water produced in the PEMFC stack, because of electrochemical reaction, evaporates and leaves the stack as vapour, the heat generated is

$$Q = (1.254 - V_{cell})IN_{cell} \tag{30}$$

Fig. 5. Control diagram of a PEMFC powered system for UPS applications.

where V_{cell} is the cell voltage and I is the stack current.

According to the Fourier's law, the heat transferred to air is

$$Q = \dot{m}_{Air} c_p \Delta T \tag{31}$$

where $\dot{m}_{Air}$ is the air mass flow rate (kg/s), c_p the heat capacity (J/kg K), and ΔT the air temperature difference between the inlet and outlet of the stack (K).

The air mass flow rate at the stack exit is given by

$$\dot{m}_{Airout} = \left[(S_{O_2} - 1)M_{O_2} + S_{O_2} \frac{1 - r_{O_2 in}}{r_{O_2 in}} M_{N_2} \right] \frac{I \cdot N_{cell}}{4F} \tag{32}$$

where M_{O_2} is the oxygen mass (kg), M_{N_2} the nitrogen mass (kg), and r_{O_2} the oxygen volume or molar fraction in the stack inlet.

Therefore, the required stoichometric radio is

$$S_{O_2} = \frac{M_{O_2} + \frac{4F(1.254 - V_{cell})}{c_p \Delta T}}{M_{O_2} + \frac{1 - r_{O_2 in}}{r_{O_2 in}} M_{N_2}} \tag{33}$$

where c_p may be expressed by an empirical relationship as $c_p = a + bT + cT^2$, and a, b and c are the empirical coefficients.

3.1.2. Hydrogen pressure controller

An increase in PEMFC operating pressure can result in higher cell voltage according to the Nernst equation and the increase in exchange current density due to increased concentration of reactant gases in the PEMFC electrodes. According to the demands of the PEMFC, this paper adopts the steady pressure equipment to control the reactant gas pressure. The hydrogen pressure controller and its mass flows controller form the cascade control. The system can also control the hydrogen pressure at about 34.5 kPa.

The mode of hydrogen supply designed is a dead-end mode, but hydrogen has to be periodically purged considering the accumulation of inert gas and water. When hydrogen is purged, the pressure will be changed. In order to protect the stack, a simple method is used: when hydrogen is purged, the power switching controller as mentioned Section 3.1.5 can control the power source of UPS to switch from PEMFC to battery.

In the PEMFC system, the relationship between the pressure (the controlled variable) and the gas flow (the controlling variable) is one-order inertia link and purely delayed segment arrayed in series, so the digital proportion integral differential (PID) control is the optimum method. Furthermore, since the control parameters K_P, T_I, and T_D are independent to each another, the parameters can be adjusted conveniently.

The PID control is used in the pressure controller, so the hydrogen output controlling variable is

$$Q_{H_2}^k = K_P e_{H_2}(kT) + \frac{T}{T_I} \sum_j^k e(jT) + \frac{T_D}{T} [e_{H_2}(kT) - e_{H_2}(kT - T)] \tag{34}$$

where $e_{H_2}(kT) = P_{H_2}^{ref}(kT) - P_{H_2}^{in}(kT)$ and T is the sampling period (ms).

3.1.3. Fuzzy controller of hydrogen mass flows

The fuzzy-PI controller input variable are the mass flow error $e(k)$, and the change of error $c(k)$ of hydrogen. The output variables of the controller are the optimal P and I gains of a subsequent PI controller device, one of them gives the proportional part K as a function of $e(k)$ and $c(k)$, and the other gives the increment ΔT, which is then integrated to provide the integral term T of the PI controller. There are the seven fuzzy subsets: positive big (PB), positive medium (PM), positive small (PS), zero (ZE), negative small (NS), negative medium (NM), and negative big (NB), have been selected for the input and output variables $e(k)$, $c(k)$, K and T. The fuzzy control rules are obtained from the behaviour analysis of the

PEMFC system. Because the rule-base represents the intelligence of the controller, the formulations must be carefully considered. Correct use of control laws according to the operating conditions can greatly improve the system stability. A fast response with a small overshoot for the PEMFC system can be achieved with proper handling of the proportional and integral parts. It is shown that the fuzzy-PI controller is more advantageous than a standard PI controller [21].

The selected control rules are described as follows:

(1) *Far from the mass flow set point*: When the output voltage is far from the set point ($e(k)$ is PB or NB), the corrective action must be strong; this means that K should be NB (or PB) while T should be zero (ZE), in order to prevent the continuous increase (or decrease) of integral term that would cause overshoots. In this case, the change of error plays little part.

The basic control rules are:

If $e(k)$ is PB, then K is PB and T is ZE;
If $e(k)$ is NB, then K is NB and T is ZE.

---

(2) *Close to the mass flow set point*: In this region, the change of error must be properly taken into account in order to ensure stability and speed of response. The goal of the fuzzy controller is to achieve a satisfactory dynamic performance with small sensitivity to parameter variations.

The control rules are:

If both $e(k)$ and $c(k)$ are ZE, then K and T are ZE;
If both $e(k)$ and $c(k)$ is negative, K and T are negative;
If both $e(k)$ and $c(k)$ is positive, K and T are positive.

3.1.4. Air supply and thermal controller

The PEMFC belongs to the low temperature stack (<100 °C) in the fuel cell family, but its operating temperature is still higher than the ambient temperature and should be maintained within an appropriate range. The operating temperature is selected according to the characteristics of the PEMFC provided by the manufacture. In this work, the best operating temperature of the PEMFC is at 50–60 °C (the maximum stack temperature is 65 °C) according to the operating temperature demands.

As mentioned above, the thermal model is nonlinear. In order to obtain good control results, in practice, when the stack temperature is less than 50 °C, the thermal controller implements the basic velocity adding digital PI control strategy. On the other hand, because three blowers are used to feed air and cool the stack together, the controller must adjust the three blowers' speed and meet the air mass flows demand of the PEMFC. When the stack temperature is more than 50 °C, a frequency-changing control strategy is employed as the air cooling control.

The air supplying and cooling control rules are: (rpm = revolutions per minutes).

If T_{stack} is less than 50 °C, then
$$Q_{O_2}^k = 1500 + K_P(T_{ref} - T(t)) + T \int (T_{ref} - T(t)) dt \ (rpm);$$
If T_{stack} is between 50 °C and 60 °C, then $Q_{O_2}^k$ = (3000–3800)+frequency-changing control (rpm);
If P_{stack} is over 330 W or T_{stack} is over 65 °C, then the PEMFC is shut down.

3.1.5. Power switching controller

The complex electrode phenomenon exists in the PEMFC and is called the charge double layer. This acts as a capacitance and gives the PEMFC stack a smooth dynamic voltage output. When the load of the PEMFC stack changes, the voltage output has an initial Ohmic voltage loss from the resistance of the fuel cell stack, as mentioned above, and then it slowly moves to a new value. When the load is suddenly increased, the fuel cell may not be able to at once provide sufficient hydrogen and air to sustain the operation under the new load condition. This can lead to temporary hydrogen and air starvation, thereby causing irreversible damage to the PEMFC stack. To avoid the hydrogen and air starvation, in this paper, a power switching controller is designed, which can control the power source of UPS to switch between PEMFC and battery according to the change rate of the power of the PEMFC stack. Transient issues associated with temporary hydrogen and air starvation can be avoided by supplying the power from the battery and slowing down the current drawn from the PEMFC through a change rate limiter of the power output.

On the other hand, in order to monitor the water balance, the open-voltage and current–voltage performance of PEMFC stack, and diagnose the operating processes taking place in the PEMFC, the measurement of the polarisation curve and the current interruption control can be used to determine if there is any problem with the PEMFC. The polarisation curve can be obtained by measuring the current and voltage of the stack on-line. The polarisation curve provides useful and sufficient information about the performance of the PEMFC. A quick measurement of the stack resistance may provide more information about the PEMFC performance. Both flooding and drying of a cell would result in a loss of voltage, that is, the stack resistance value will be changed. Therefore, the water balance can be reflected by the stack resistance.

One of the methods to measure the resistance in the PEMFC stack is the current interruption method. In this method, the current is interrupted for a very short period, which is determined by the current value of the stack, and resulting voltage gain is observed and calculated. The difference between the stack voltage before and after the current interruption, divided by the current, is the stack resistance R_{Ohmic}, which is expressed by the following equation. When the current is interrupted, the power switch controller can control the power source of UPS to switch from PEMFC to battery.

$$R_{Ohmic} = \frac{\Delta V_R}{I} \tag{35}$$

To realise the operation as mentioned above, the intelligent control rules are as follows. As shown in Fig. 3, $u_{k_1} = 1$ means that the SCR$_1$ turns on; $u_{k_1} = 0$ means that the SCR$_1$ turns off; $u_{k_2} = 0$ means that SCR$_2$ turns off; $u_{k_2} = 1$ means that the SCR$_2$ turns on.

If the change of load $\frac{dP_{stack}}{dt} < 50\%$, then $u_{k_2} = 1$ and $u_{k_3} = 0$;

If the change of load $\frac{dP_{stack}}{dt} \geqslant 50\%$, then $u_{k_2} = 0$ and $u_{k_3} = 1$;

If the battery voltage $V_{Battery}$ is less 30 V and the utility input voltage is less than 160 V, then $u_{k_2} = 1$ and $u_{k_3} = 1$ (PEMFC charges battery);

If the current interrupt is executed, then $u_{k_2} = 0$ and $u_{k_3} = 1$;

If the hydrogen is purged, then $u_{k_2} = 0$ and $u_{k_3} = 1$;

If the PEMFC is failure, then $u_{k_1} = 0$ and $u_{k_2} = 1$.

3.2. Control of power converters in hybrid UPS system

Using the concept of feedback control, the power converters can be built into the close-loop system, to improve the output accuracy and dynamic performances. In order to make power converters meet the demands of stable and dynamic performance specifications, the compensation network, or, the voltage or current controller must be designed very well. The controllers design has many methods, such as using the time-domain method or frequency-domain method of the classical control theory, the pole placement method, and adaptive control of modern control theory, the fuzzy control and neural network control of intelligent control technologies, and so on.

In this paper, in the opinion of adopting the matured technology, the Bode diagram approach of the frequency-domain method is utilised to design the controllers of power converters in hybrid UPS system.

3.2.1. Control of AC/DC rectifier

As shown in Fig. 6, there are two controllers in the AC/DC rectifier: one is the current controller $G_I(s)$, another is the voltage controller $G_V(s)$.

According to computing and designing of the Bode diagram Method, their transfer functions are given by

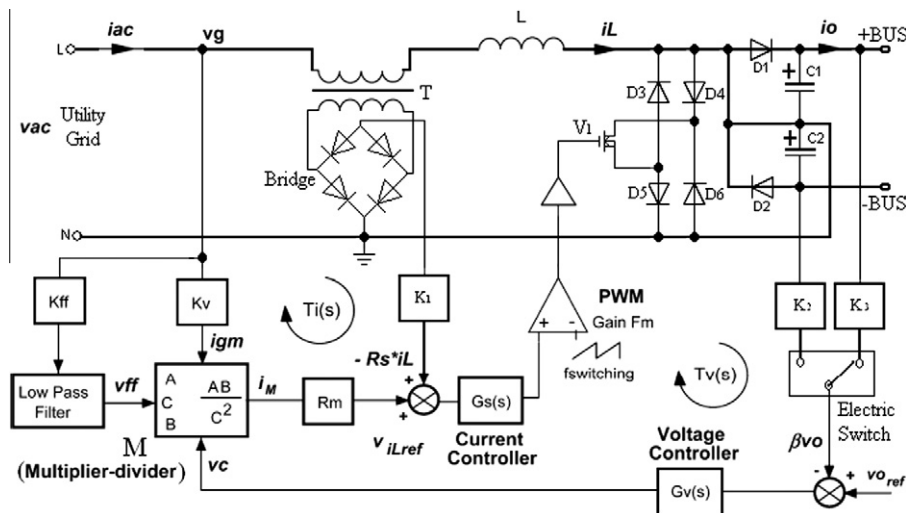$$G_V(s) = \frac{K_V}{1 + T_V s} = \frac{2.238}{1 + 0.0022s} \tag{36}$$

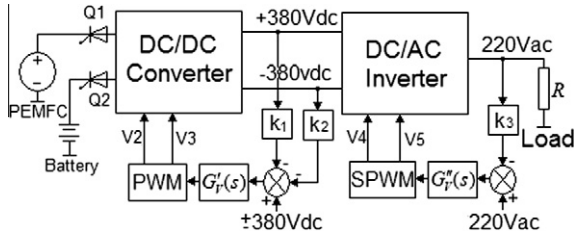Fig. 6. Schematic principle diagram of boost AC/DC rectifier.

Fig. 7. Schematic principle diagram of DC/DC and DC/AC power converters.

$$G_I(s) = K_I\left(1 + \frac{1}{T_I s}\right) = 2.0 \times \left(1 + \frac{1}{0.0003s}\right) \tag{37}$$

3.2.2. Control of DC/DC converter

As shown in Fig. 7, $G'_V(s)$ shows the voltage controller of DC/DC converter. According to computing and designing of the Bode diagram Method, its voltage controller of DC/DC converter is determined by

$$G'_V(s) = \frac{K'_V}{1 + T'_V s} = \frac{1.5}{1 + 0.0015s} \tag{38}$$

3.2.3. Control of DC/AC inverter

As shown in Fig. 7, $G''_V(s)$ shows the voltage controller of DC/AC inverter. Because the control method used in this paper is the voltage transient control, according to computing and designing of the Bode diagram Method, its voltage controller is a lead-lag compensation controller, which transfers function can be written as follows:

$$\begin{aligned} G''_V(s) &= \frac{K''_V(1 + \tau_1 s)(1 + \tau_2 s)}{s(1 + \tau_3 s)(1 + \tau_4 s)} \\ &= \frac{100(1 + 0.00169s)(1 + 0.000108s)}{s(1 + 7.9 \times 10^{-6}s)(1 + 4.7 \times 10^{-6}s)} \end{aligned} \tag{39}$$

4. Experimental setup, results and discussion

4.1. Experimental setup

The performances of the proposed control strategies of PEMFC generating system and hybrid UPS power converters are tested by building an experimental setup with the following specifications: the input voltage of the utility grid = 160–275 V AC, the output voltage frequency = 50 Hz ± 5%, the PEMFC/battery rated voltage = 36 V DC, the output power of the load = 286 W. The
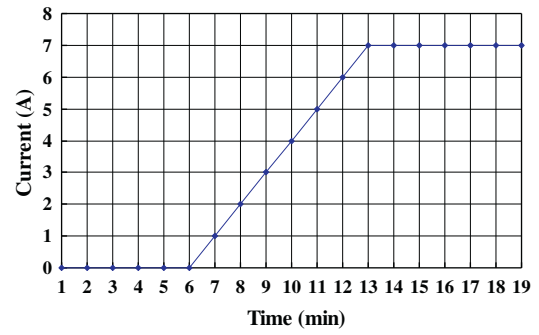
[(a) Current]
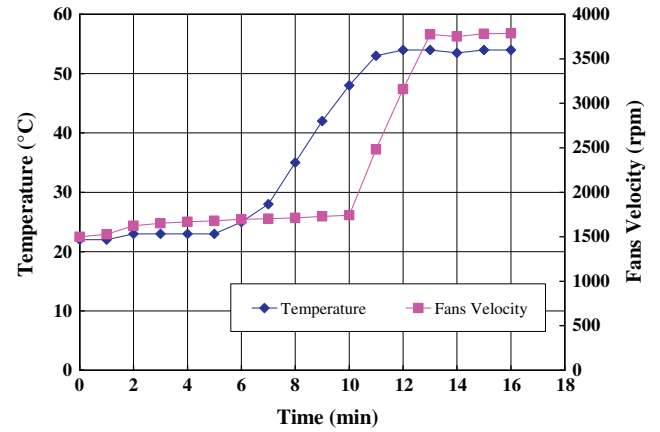
[(b) Temperature and blower speed]

Fig. 9. Stack temperature and blower speed when UPS load (current) changes.

experimental load is a DELL™ computer, whose model is HP-U2106F3, and the maximum input power is 213 W, and a monitor, whose model is E772p with power of 73 W. Moreover, a lamp box is used as the supplementary load. Agilent Technologies DSO6034A Oscilloscope, TEKTRONIX AM503 Current Probe Amplifier and P5120 High Voltage Differential probe are employed as measurement equipments.

Because the PEMFC stack is a self-humidified, air-breathing and air-cooling together, some parameters are confidential to the manufacturer of the stack such as the anode volume, cathode volume and so on, we have to do some experiments, and no simulations. The basic experimental conditions of PEMFC are: hydrogen input flow of 5.18×10^{-6} mol/s, number of cells of 63, Faraday's constant of 96,485 C/mol, universal gas constant of 8.314 J/mol K, k_r the
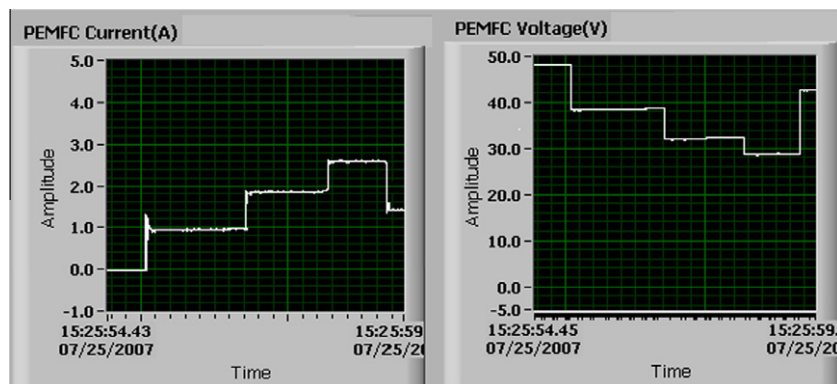

Fig. 8. Current and voltage of PEMFC when UPS load changes.
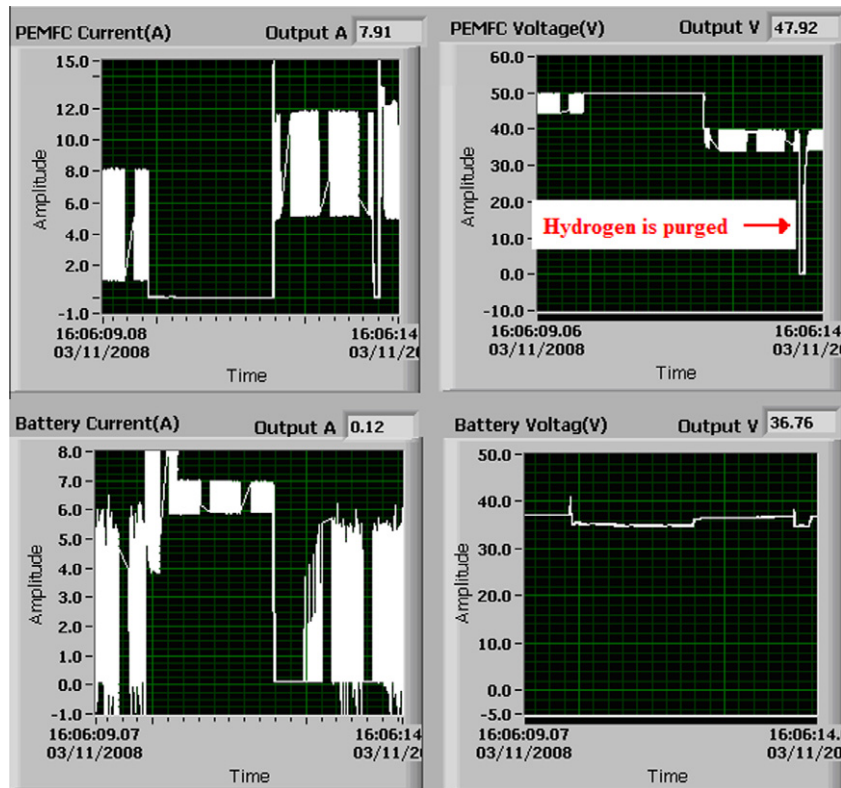
Fig. 10. Power supply switching from PEMFC to battery when the load of UPS changes sharply (over 250%) or hydrogen is purged.
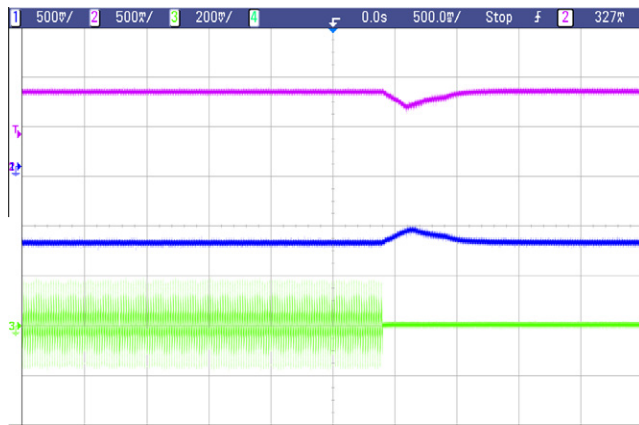

Fig. 11. Output voltage (ch1, ch2) of AC/DC rectifier and DC/DC converter when the utility input failures (ch3) and PEMFC supplying power source.

modelling constant of 1.63×10^{-4}, fuel cell absolute temperature of 333 K, fuel cell internal resistance of 6.29 Ω.

In the hybrid UPS system, the parameters of AC/DC rectifier are the operating frequency is 20 kHz; L_1 = 2 mH; C_1 = 440 µF; V_{BUS} = 380 V; R = 1.84 Ω; and V_M = 3 V. When the current is under the condition of the continuous, the parameters of DC/DC converter are the operating frequency is 50 kHz; V_{in} = 36 V; N = 32/3; T_S = 20 µs; and L_2 = 0.65 mH. The parameters of DC/AC inverter are the operating frequency is 20 kHz; L_3 = 5 mH; C_3 = 2.2 µF; V_{BUS} = 380 V; R = 33.66 Ω; and $V'_M = 3$ V.

In the hybrid UPS system, a set of three 12 V, 7.2Ah PANASONIC batteries with high discharge current have been chosen for this application, which type and specifications are LC-R127R2CH, 12 V/7.2Ah/20HR, respectively. On the other hand, one may use

15 series-connected supercapacitors with the main specifications as 1000 F (±20%), control voltage of 2.5 V, and maximum current of 150 A.

4.2. Experimental results and discussion

Experimental study has been conducted on the designed UPS with backup PEMFC and battery. The proposed intelligent comprehensive control strategies have been implemented in the PEMFC generating system. Based on the intelligent comprehensive control, the output voltage and current of the PEMFC stack can be easily controlled according to the load change of the UPS, as shown in Fig. 8.

With the increase of the load, the temperature of PEMFC stack will go up. Because of the adjustment of thermal controller, the temperature of the stack will keep in the range of 50–60 °C, as shown in Fig. 9. In general, higher operating temperature is desirable due to decreased mass transport limitation and increased electrochemical reaction rate; at the same time, high temperatures may lead to increased mass transport losses due to the increases in water vapour. Therefore, in this experiment, the stack temperature is controlled within 50–60 °C, in order to keep the water balance and reduce the effect of the internal resistance or Ohmic losses.

The experimental results reveal that when the external load has a sudden change, however, the hydrogen cannot be fed fast enough to the PEMFC stack. When the load of the UPS suddenly changes, for example, from 60 W to 210 W, the output voltage of the PEMFC stack goes down quickly and makes the UPS shut down, resulting in hydrogen and air starvation that may damage the PEMFC stack. To supply enough power to the external load and protect the PEMFC stack, the UPS system keeps adopting the lead-acid battery for protecting the PEMFC from excessive use of the PEMFC and to feed power smoothly to the external load. As shown in Fig. 10, the PEMFC stack can supply the UPS for a long time in the normal condi-
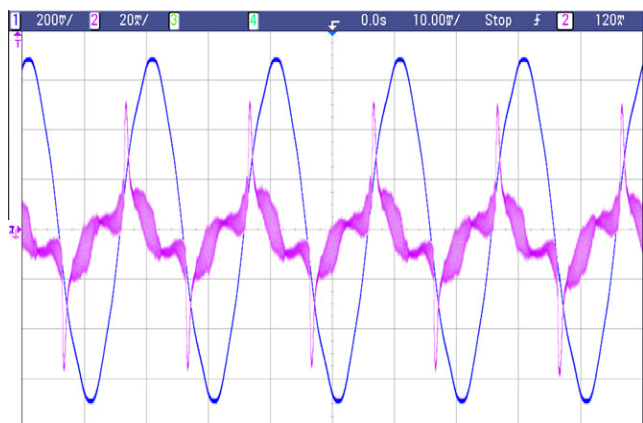
Fig. 12. Input voltage (ch1) and current (ch2) of UPS when utility grid is normal.
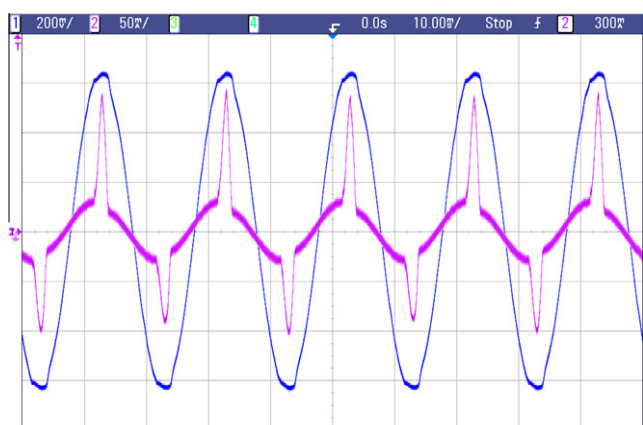

Fig. 13. Output voltage (ch1) and current (ch2) of UPS supplying power with PEMFC.

tions, and when the load of the UPS sharply changes, the power switch controller can switch from PEMFC to battery. After a period of time, when the PEMFC runs stably, the power source of the UPS can be switched back from battery to PEMFC. In Fig. 10, when the hydrogen is purged, the power switch controller can switch from PEMFC to battery.

The change of output voltage of AC/DC rectifier and DC/DC converter, and the regulation of the BUS DC voltage are reported, as shown in Fig. 11, when the utility input failures and PEMFC supplies UPS. Fig. 12 plots the experimental waveform of the input voltage and current of UPS when utility grid is normal, which shows that the AC/DC rectifier is of the function of the power factor regulation. The output voltage and current of the DC/AC inverter can be observed in Fig. 13 when UPS is supplied power source by PEMFC.

5. Conclusion

This paper presents the dynamic models and controllers of a hy-brid UPS system with backup PEMFC and battery power sources, in which cost effective and practical DC/DC converter, DC/AC inverter, AC/DC rectifier and PEMFC generating system are designed to feed a typical computer load. The proposed intelligent comprehensive controller of PEMFC includes a power tacking controller, a hydro-gen pressure controller, a hydrogen mass flows controller, an air supply and thermal controller, and a power switching controller. The designed topologies of power converters for hybrid UPS sys-tem allow us to process the energy produced by the PEMFC inde-pendently and in parallel to that of batteries. An experimental evaluation has been carried out, and the performances have been tested. The experimental results show that the designed control-lers of power converters and PEMFC are practical for industry applications.

References

[1] Jia JB, Cham YT, Wang Y, Lewis F. The electrical dynamic response study of PEMFC as a backup power supply. In: Proc. IEEE international conference on control and automation; 2007. ThB 1–4.
[2] Gonzales J, Tamizhmani G. High efficiency fuel cell based uninterruptible power supply for digital equipment. J Power Sources 2006;153:151–6.
[3] Varkaraki E, Lymberopoulos N, Zachariou A. Hydrogen based emergency back-up system for telecommunication applications. J Power Sources 2003;118:14–22.
[4] Moth K, Schmidt JD. APC fuel cell solution for extended run time UPS. The 27th international telecommunications conference, INTELEC '05; September 2005. p. 361–5.
[5] Hajizadeh A, Golkar MA. Intelligent power management strategy of hybrid distributed generation system. J Electr Power Energy Syst 2007;29:783–95.
[6] Han JS, Park ES. Direct methanol fuel-cell combined with a small backup battery. J Power Sources 2002;112:477–83.
[7] Yang YP, Wang FC, Changb HP, Ma YW, Weng BJ. Low power proton exchange membrane fuel cell system identification and adaptive control. J Power Sources 2007;164:761–71.
[8] Xue X, Tang J, Sammes N, Ding Y. Model-based condition monitoring of PEM fuel cell using Hotelling T2 control limit. J Power Sources 2006;162:388–99.
[9] Jiang ZH, Gao LJ, Blackwelder MJ, Dougal RA. Design and experimental tests of control strategies for active hybrid fuel cell/battery power sources. J Power Sources 2004;130:163–71.
[10] Lin M, Cheng Y, Lin M, Yen S. Evaluation of PEMFC power systems for UPS base station applications. J Power Sources 2005;140:346–9.
[11] Choi W, Howzeb JW, Enjeti P. Fuel-cell powered uninterruptible power supply systems: design considerations. J Power Sources 2006;157:311–7.
[12] Varkaraki E, Lymberopoulos N, Zoulias E, Guichardot D, Poli G. Hydrogen-based uninterruptible power supply. Int J Hydrogen Energy 2007;32:1589–96.
[13] Bernardinis AD, Péra MC, Garnier J, Hissel D, Coquery G, Kauffmann JM. Fuel cells multi-stack power architectures and experimental validation of 1 kW parallel twin stack PEFC generator based on high frequency magnetic coupling dedicated to on board power unit. Energy Convers Manage 2008;49(8):2367–83.
[14] Haraldsson K, Wipke K. Evaluating PEM fuel cell system models. J Power Sources 2004;126:88–97.
[15] Zhan YD, Zhu JG, Guo YG, Wang H. Comprehensive control of proton exchange membrane fuel cell as backup power supply for UPS. In: Proc 27th Chinese control conference; 2008. p. 646–51.
[16] Vahidi A, Stebloweropolou A, Peng H. Model predictive control for starvation prevention in a hybrid fuel cell system. In: Proc 2004 American control conference; 2004. p. 834–9.
[17] Xu DH. Modelling and control of power electronics system. Beijing: China Machine Press; 2006.
[18] Mierlo JV, Bossche PVD, Maggetto G. Models of energy sources for EV and HEV: fuel cells, batteries, supercapacitors, flywheels and engine-generators. J Power Sources 2004;128:76–89.
[19] Horizon Technology, 300W fuel cell stack operating instruments. <www.horizonfuelcell.com>.
[20] Barbir F. FEM fuel cell: theory and practice. New York: Elsevier Academic Press; 2005.
[21] Zhan YD, Zhu JG, Guo YG, Jin JX. Control of proton exchange membrane fuel cell based on fuzzy logic. In: Proc 26th Chinese control conference; 2007. p. 2015–9.